Use of SDS Micelles To Stabilize a Ternary Intermediate in the Reaction of Ferrioxamine B and 1,10-Phenanthroline

Edwin G. Olmstead, Jr.,† Suzanne W. Harman, Pek Lee Choo, and Alvin L. Crumbliss*

Department of Chemistry, Duke University, Box 90346, Durham, North Carolina 27708-0346

Received August 1, 2001

Spectrophotometric measurements of the reaction of ferrioxamine B ($FeHDFB^+$) with 1,10-phenanthroline (phen) reveal the presence of a ternary intermediate complex in both aqueous solution and an aqueous solution of 0.16 M sodium dodecyl sulfate (SDS). The stoichiometry of the intermediate is $Fe(H_2DFB)(phen)^{2+}$ on the basis of a Schwarzenbach analysis of spectrophotometric data obtained at variable pH and phen concentrations. The ternary complex formation constant for the reaction $FeHDFB^+ + H^+ + phen \rightleftarrows Fe(H_2DFB)(phen)^{2+}$ is $\log K = 6.96$ in aqueous solution and $\log K = 8.64$ in aqueous 0.16 M SDS. The enhanced stability of $Fe(H_2DFB)(phen)^{2+}$ in micellar solution was analyzed in terms of the pseudophase ion-exchange (PPIE) model of micellar reactions. The association constants for the binding of each reactant to the micellar pseudophase were measured by ultrafiltration. According to PPIE model calculations, the enhanced stability of $Fe(H_2DFB)(phen)^{2+}$ in micellar SDS arises from a proximity effect created by the high local concentrations of reactants in the micellar pseudophase. The calculations also indicate that an inhibitory medium or compartmentalization effect is operative since the observed micellar enhancement is much smaller than predicted by the PPIE model. The micellar stabilization of the $Fe(H_2DFB)(phen)^{2+}$ intermediate and the overall conversion of $FeHDFB^+$ to $Fe(phen)_3^{2+}$ are discussed as a possible model system for siderophore iron release in microbial organisms.

Introduction

Iron is an essential nutrient for microbial growth. However, its bioavailability is severely limited in most environments by the insolubility of iron(III). Microorganisms overcome the problem of iron scarcity by secreting chelating agents, known as siderophores, that possess a high affinity and specificity for iron(III).[1−5] Once iron has been solubilized by siderophore chelation and transported to the cell, iron release must occur, either at the cell surface or interior. The mechanisms of iron release from siderophores, which vary with siderophore and organism, are topics of continuing investigation. The reduction of iron has been postulated to play a key role in the release of iron from some siderophores.[4,6−11] However, since at pH 7 the redox potentials of many hexadentate siderophores are too negative to be accessible to biological reducing agents, additional processes must be operative.[4,8] For these siderophores, it is suspected that a positive shift in redox potential is created through hydrolysis of the siderophore backbone,[12−14] ligand protonation,[15,16] ternary complex formation,[4] or a coupling of the redox process with an Fe(II) chelation reaction.[8]

Our current interest in this process is focused on the role that the cellular membrane environment may play in the removal of iron from its siderophore complex. A simple biomimetic model system consisting of a positively charged siderophore complex (ferrioxamine B; $FeHDFB^+$), a hydrophobic iron(II) chelator (1,10-phenanthroline; phen), and sodium dodecyl sulfate (SDS) micelles is presented here. Deferriferrioxamine B (**I**, H_4DFB^+) is a linear trihydroxamic acid produced by some species of *Nocardia* and *Streptomyces*[17] and has a high affinity for Fe(III) ($\log \beta_{Fe(III)} = 30.60$)[18] that is diminished by 20 orders of magnitude upon reduction to Fe(II) ($\log \beta_{Fe(II)} = 10.0$).[8] The

* Corresponding author. E-mail: alc@chem.duke.edu. Fax: 919-660-1605.

† Current address: Department of Chemistry, Gordon College, 255 Grapevine Road, Wenham, MA 01984.

(1) Winkelmann, G.; van der Helm, D.; Neilands, J. B. *Iron Transport in Microbes, Plants and Animals*; VCH Publishers: New York, 1987.
(2) Matzanke, B. F.; Müller-Matzanke, G.; Raymond, K. N. Siderophore-Mediated Iron Transport. In *Iron Carriers and Iron Proteins*; Loehr, T. M., Ed.; VCH: New York, 1989; pp 1−122.
(3) Winkelmann, G. *CRC Handbook of Microbial Chelates*; CRC Press: New York, 1991.
(4) Albrecht-Gary, A. M.; Crumbliss, A. L. The Coordination Chemistry of Siderophores: Thermodynamics and Kinetics of Iron Chelation and Release. In *Metal Ions in Biological Systems*; Sigel, A., Sigel, H., Eds.; Marcel Dekker: New York, 1998; Vol. 35.
(5) Albrecht-Gary, A. M.; Crumbliss, A. L. Siderophore-Mediated Microbial Iron Bioavailability: A Paradigm for Specific Metal Ion Transport. In *Scientific Bridges for 2000 and Beyond*, TEC and DOC eds.; Institut de France, Académie des Sciences: Paris, 1999; p 73.
(6) Emery, T. Reductive Mechanisms of Iron Assimilation. In *Iron Transport in Microbes, Plants and Animals*; Winkelmann, G., van der Helm, D., Neilands, J. B., Eds.; VCH: New York, 1987; pp 235−250.
(7) Crumbliss, A. L. Aqueous Solution Equilibrium and Kinetic Studies of Iron Siderophore and Model Siderophore Complexes. In *CRC Handbook of Microbial Chelates*; Winkelmann, G., Ed.; CRC Press: Boca Raton, FL, 1991; pp 177−233.
(8) Spasojević, I.; Armstrong, S. K.; Brickman, T. J.; Crumbliss, A. L. *Inorg. Chem.* **1999**, *38*, 449−454.
(9) Barchini, E.; Cowart, R. E. *Arch. Microbiol.* **1996**, *166*, 51−57.
(10) Vartivarian, S. E.; Cowart, R. E. *Arch. Biochem. Biophys.* **1999**, *364*, 74−82.
(11) Yun, C.-W.; Ferea, T.; Rashford, J.; Ardon, O.; Brown, P. O.; Botstein, D.; Kaplan, J.; Philpott, C. C. *J. Biol. Chem.* **2000**, *275*, 10709−10715.
(12) O'Brian, I. G.; Cox, G. B.; Gibson, F. *Biochim. Biophys. Acta* **1971**, *237*, 537−549.
(13) Cooper, S. R.; McArdle, J. V.; Raymond, K. N. *Proc. Natl. Acad. Sci. U.S.A.* **1978**, *75*, 3551−3554.
(14) Brickman, T. J.; McIntosh, M. A. *J. Biol. Chem.* **1992**, *17*, 12350−12355.
(15) Lee, C.-W.; Ecker, D. J.; Raymond, K. N. *J. Am. Chem. Soc.* **1985**, *107*, 6920−6923.
(16) Helman, R.; Lawrence, G. D. *Bioelectrochem. Bioenerg.* **1989**, *22* (276), 187−196.
(17) Müller, G.; Raymond, K. N. *J. Bacteriol.* **1984**, *160*, 304−312.

10.1021/ic0008621 CCC: $20.00
Published on Web 09/13/2001

kinetics and mechanism of Fe(III) release from ferrioxamine B at low pH have been investigated.[19,20] Aqueous micellar SDS was found to accelerate the dissociation of ferrioxamine B through a process whereby the siderophore is bound to the anionic surface of the micelle in a region of relatively high H^+ concentration.[21]

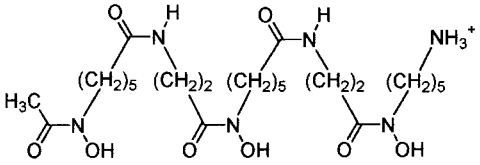

I - Deferriferrioxamine B (H_4DFB^+)

In contrast with ferrioxamine B, the tris(1,10-phenanthroline)-iron(III) complex ($\log \beta = 14.1$)[22] is stabilized by reduction to its iron(II) analogue ($\log \beta = 21.0$).[22] In our model system, the phen ligand can promote the reductive release of iron from $FeHDFB^+$ in two ways. First, if a ternary complex is formed, the greater affinity of phen for iron(II) will create a positive shift in the iron(III/II) redox potential. Second, by coupling the iron reduction process to the subsequent formation of the stable $Fe(phen)_3^{2+}$ complex, the overall reaction becomes more exergonic and the equilibrium is shifted toward increased product formation.

Micelles are commonly used as biomimetic models for membranes[23,24] and are also known to dramatically alter the rates and equilibria of chemical reactions.[25−34] To model the micellar effects on our reaction, we used a modification of the original micelle pseudophase model,[35] called the pseudophase ion-exchange (PPIE) model.[27,29,36] Pseudophase models treat aqueous micellar aggregates as a two-phase system comprised of the bulk and micelle phases. In the PPIE model, neutral solute−micelle interactions are treated as a simple binding process with a characteristic binding constant, and ionic solute−micelle interactions are treated as a selective ion-exchange process with a specific ion-exchange constant.

Alterations in the rate and equilibria of reactions in the presence of micelles can arise from three effects. The first is a "proximity" effect, where increases in the reaction rate and shifts in equilibria arise when the "local" concentrations of reactants and products in the micellar pseudophase are significantly larger than their bulk solution concentrations. The second is a "medium" effect, which causes the rate and equilibrium constants in the micellar pseudophase to be substantially different from those in aqueous solution. The third is a "compartmentalization" effect in which the observed rate and equilibrium constants are smaller than expected because reactants are localized in different regions of the micellar aggregates.

In the classical pseudophase and PPIE models, the magnitude of the proximity effect is calculated from the local concentrations of reactants and products in the micellar pseudophase. Any residual differences in rate or equilibria are usually attributed to the medium effect. However, because these models view the micellar aggregate as a single homogeneous "phase", they cannot distinguish the medium effect from the compartmentalization effect. Alternative approaches have been developed in which the combined micellar effects are expressed simply in terms of the stabilization of the transition state of the reaction;[37−40] however, there are relatively few published reports in which these models have been applied to experimental data.

Here, we present the effect of SDS micellar aggregates on the reaction of $FeHDFB^+$ with phen. In this reaction, we observe the formation of a ternary intermediate complex that is stabilized in micellar SDS. The stoichiometry of this ternary intermediate is identified, and the magnitude of the micellar proximity effect is estimated from the PPIE model. The results of this study illustrate a viable pathway in which the cell membrane environment may facilitate the reductive release of iron from a siderophore complex.

Experimental Section

Reagent Preparation. An iron(III) stock solution containing 0.105 M Fe^{3+} and 0.100 M H^+ was prepared from recrystallized iron(III) perchlorate (G. F. Smith) and perchloric acid (Fisher, 70%) and standardized by the absorbance at 240 nm.[41] Sodium dodecyl sulfate (ICN, ultrapure >99%), deferriferrioxamine B mesylate (Sigma, 95%), 1,10-phenanthroline (Aldrich, >99%), tris(hydroxymethyl)aminomethane acetate (Sigma, Trizma acetate, reagent), bis(2-hydroxyethyl)iminotris-(hydroxymethyl)methane (ICN, Bis-Tris, >99%), sodium nitrate (Aldrich, analytical reagent), nitric acid (Mallinckrodt, analytical reagent), and sodium hydroxide (Fisher) were used as supplied without any further purification. In all experiments, doubly distilled or 18 MΩ water obtained by ion-exchange purification was used.

Standard HNO_3 solutions were prepared by dilution of 70% HNO_3 and standardization with 0.1 M NaOH. Sodium nitrate stock solutions were standardized by eluting an aliquot through a Dowex 50W-X8 cation-exchange resin in the H^+ form and titrating the eluant with a standard 0.1 M NaOH solution. Stock buffer solutions (0.50 M) were made from $Tris^+$, $Bis\text{-}Tris^+$, or sodium acetate and were adjusted to the desired pH with HNO_3. Ferrioxamine B solutions were prepared by dissolving a 5% excess of deferriferrioxamine mesylate in a small volume of water, adding 125 mL of 0.2 M HNO_3, and introducing a

(18) Martell, A. E.; Smith, R. M. *Critical Stability Constants*; Plenum Press: New York, 1977; Vol. 3.
(19) Monzyk, B.; Crumbliss, A. L. *J. Am. Chem. Soc.* **1982**, *104*, 4921−4929.
(20) Biruš, M.; Bradić, Z.; Krznarić, G.; Kujundžic, N.; Pribanić, M.; Wilkins, P. C.; Wilkins, R. G. *Inorg. Chem.* **1987**, *26*, 1000−1005.
(21) Batinić-Haberle, I.; Spasojević, I.; Crumbliss, A. L. *Inorg. Chem.* **1994**, *33*, 3151−3158.
(22) Martell, A. E.; Smith, R. M. *Critical Stability Constants*; Plenum Press: New York, 1975; Vol. 2.
(23) Fendler, J. H. *Membrane Mimetic Chemistry*; John Wiley & Sons: New York, 1982.
(24) Fendler, J. H. *Chem. Eng. News* **1984**, *Jan. 2*, 25−38.
(25) Cordes, E. H.; Dunlap, R. B. *Acc. Chem. Res.* **1969**, *2*, 329−337.
(26) Fendler, J. H.; Fendler, E. J. *Catalysis in Micellar and Macromolecular Systems*; Academic Press: New York, 1975.
(27) Romsted, L. S. Micellar Effects on Reaction Rates and Equilibria. In *Surfactants in Solution*; Mittal, K. L., Lindman, B., Eds.; Plenum Press: New York, 1984; Vol. 2, pp 1015−1068.
(28) Bunton, C. A.; Savelli, G. Organic Reactivity in Aqueous Micelles and Similar Assemblies. In *Advances in Physical Organic Chemistry*; Gold, V., Bethell, D., Eds.; Academic Press: New York, 1986; Vol. 22, pp 213−309.
(29) Bunton, C. A.; Nome, F.; Quina, F. H.; Romsted, L. S. *Acc. Chem. Res.* **1991**, *24*, 357−364.
(30) Hebrant, M.; Francois, N.; Tondre, C. *Colloids Surf., A* **1998**, *143*, 77−88.
(31) Tondre, C.; Hebrant, M. *J. Mol. Liq.* **1997**, *72*, 279−294.
(32) Hebrant, M.; Toumi, C.; Tondre, C.; Rogue, J. P.; Leydet, A.; Boyer, B. *Colloid Polym. Sci.* **1996**, *274*, 453−460.
(33) Cierpiszewski, R.; Hebrant, M.; Szymanowski, J.; Tondre, C. *J. Chem. Soc., Faraday Trans.* **1996**, *92*, 249−255.
(34) Szymanowski, J.; Tondre, C. *Solvent Extr. Ion Exch.* **1994**, *12*, 873−905.
(35) Berezin, I. V.; Martinek, K.; Yatsimirskii, A. K. *Russ. Chem. Rev.* **1973**, *42*, 787−802.
(36) Quina, F. J.; Chalmovich, H. *J. Phys. Chem.* **1979**, *83*, 1844−1850.
(37) Hall, D. G. *J. Phys. Chem.* **1987**, *91*, 4287−4297.
(38) Davies, D. M.; Gillitt, N. D.; Paradis, P. M. *J. Chem. Soc., Perkin Trans. 2* **1996**, 659−666.
(39) Davies, D. M.; Foggo, S. J. *J. Chem. Soc., Perkin Trans. 2* **1998**, 247−251.
(40) Muriel-Delgado, F.; Jiménez, R.; Gómez-Herrera, C.; Sánchez, F. *Langmuir* **1999**, *15*, 4344−4350.
(41) Bastian, R.; Weberling, R.; Palilla, F. *Anal. Chem.* **1956**, *28*, 459−462.

stoichiometric amount of $Fe(ClO_4)_3$ stock solution. After being stirred for 30 min, the solution was neutralized with NaOH, a 25 mL aliquot of the stock buffer solution was added, and the solution was diluted to a 250 mL volume. For micellar solutions, solid SDS was dissolved in the $FeHDFB^+$ solution just prior to the addition of phen.

Equipment and Procedures. pH Measurements. All pH measurements were made with a Corning 250 pH/ion meter with a Corning general purpose glass electrode. To avoid a drift in the electrode response due to the precipitation of potassium dodecyl sulfate in the liquid junction of the electrode,[42,43] the usual KCl fill solution was replaced by a 5 M NH_4Cl solution. The pH meter was calibrated at pH 7 and 4 with standard Fisher Scientific buffer solutions before each series of measurements. Between each pH measurement, the electrode was stored in the pH 7 calibration buffer solution and the pH readings were monitored to detect any drift in electrode response. These pH readings were found to remain constant at pH 7.00 ± 0.02.

Equilibrium Measurements. Spectrophotometric measurements of the micellar SDS reactions were recorded with a Beckman Acta III spectrophotometer interfaced to an electronic data acquisition system from On-Line Instruments Systems (OLIS). Phenanthroline and proton stoichiometries for reaction 9 were determined by a phenanthroline and a pH spectrophotometric titration at 525 nm. In the phenanthroline titration, solid phenanthroline was added incrementally to a solution containing $FeHDFB^+$ in micellar SDS. In the H^+ titration, the reaction solution was prepared by dissolving solid SDS and solid phen in an $FeHDFB^+$ solution and then titrating with small increments of 0.200 M HNO_3. The dilution effect of the SDS addition was measured by recording the absorbance at 430 nm before and after SDS addition. The volume of each HNO_3 addition was recorded and used to apply a dilution correction to the absorbance readings. In both titrations, the $FeHDFB^+$/micellar SDS solution was prepared with the following composition: $[Fe^{3+}]_{tot} = 2.87 \times 10^{-4}$ M, $[H_4DFB^+]_{tot} \cong 3.3 \times 10^{-4}$ M, 0.16 M SDS, and 0.1 M $NaNO_3$. For the phen titration, the buffer was 0.05 M Bis-Tris at an initial pH of 6.30 and data were collected at the following [phen] and pH values: (i) 0 mM, 6.30; (ii) 1.0 mM, 6.31; (iii) 2.5 mM, 6.32; (iv) 5.0 mM, 6.33; (v) 7.5 mM, 6.34; (vi) 10 mM, 6.35; and (vii) 12.5 mM, 6.36. The slight increase in pH with phen addition results from the partial protonation of phen ($pK_a = 4.93$, 25 °C, $I = 0.1$ M).[22] In the H^+ titration, the buffer was 0.05 M Tris, $[phen]_{tot} = 0.0125$ M, and the data were collected at 25.0 ± 0.1 °C at the following pH values: (i) 7.22, (ii) 7.13, (iii) 6.96, (iv) 6.76, (v) 6.59, (vi) 6.40, (vii) 6.30, (viii) 6.23, and (ix) 6.03.

Spectrophotometric measurements of the aqueous reactions were recorded with a Cary Bio 100 spectrophotometer. In these experiments, two series of 50 mL solutions with differing pH and [phen] values were prepared. In both series, the $FeHDFB^+$/phen reaction mixtures had the following composition: $[Fe^{3+}]_{tot} = 3.05 \times 10^{-4}$ M, $[H_4DFB^+]_{tot} \cong 3.3 \times 10^{-4}$ M, 0.1 M $NaNO_3$, and 0.05 M sodium acetate buffer. In the first series, a control solution containing no phen was prepared with a pH of 4.54; for all other solutions in this series, $[phen]_{tot} = 0.0100$ M and the pH values were (i) 5.42, (ii) 5.25, (iii) 4.84, (iv) 4.59, (v) 4.46, and (vi) 4.38. In the second series, the buffer was initially adjusted to pH 4.54. After phen addition, solutions contained the following [phen] and pH values: (i) 0 mM, 4.54; (ii) 1.0 mM, 4.57; (iii) 2.0 mM, 4.58; (iv) 4.0 mM, 4.64; (v) 6.0 mM, 4.68; (vi) 8.0 mM, 4.72; and (vii) 10.0 mM, 4.76. The significant change in solution pH arises from the protonation of phen. For the Schwarzenbach plot analysis, the concentration of unprotonated phen was calculated from the pK_a of phen (4.93, 25 °C, $I = 0.1$ M)[22] and the measured change in pH. Immediately upon the dissolution of phen, all reaction mixtures were placed in a temperature bath maintained at 25.0 ± 0.1 °C. Spectra were collected approximately 1 h after the addition of phen. Comparison of these spectra to subsequent measurements verified that reaction 9 reaches equilibrium prior to 1 h.

For each series of equilibrium spectra, a rank analysis was performed to determine the number of light-absorbing species present. For the rank analysis, the matrix triangularization method of Wallace and Katz was employed.[44] However, instead of assuming that the error in absorbance is a constant, the elements of the error matrix were calculated as $s_{ij} = 0.43429\Delta T \times 10^{A_{ij}}$, assuming a value of ΔT of 0.005.[45]

Kinetic Measurements. Kinetic measurements were performed at 25.0 ± 0.1 °C using a Beckman DU spectrophotometer equipped with an Aminco stopped-flow apparatus and an OLIS electronic data acquisition system. A ferrioxamine B reactant solution ($[Fe^{3+}]_{tot} = 3.0 \times 10^{-4}$ M, $[H_4DFB^+]_{tot} \cong 3.3 \times 10^{-4}$ M, 0.04 M SDS, 0.1 M $NaNO_3$, 0.05 M Tris acetate, pH 4.75) was mixed with a phen reactant solution (0.010 M phen, 0.04 M SDS, 0.05 M Tris acetate, pH 4.75) to give a reaction mixture with the following composition: $[Fe^{3+}]_{tot} = 1.5 \times 10^{-4}$ M, $[H_4DFB^+]_{tot} \cong 1.65 \times 10^{-4}$ M, $[phen]_{tot} = 0.0050$ M, 0.04 M SDS, 0.05 M $NaNO_3$, 0.05 M Tris acetate, pH 4.75. Absorbance data were collected at 400 and 510 nm, where pseudo-first-order kinetic behavior was observed for at least five half-lives. The reported pseudo-first-order rate constants are an average of three kinetic determinations.

Ultrafiltration Experiments. Background information on the ultrafiltration methods used, data analysis, and the derivation of the equations are given in Supporting Information. Ultrafiltration experiments were performed with Amicon 1000 MWCO filters in an Amicon model 8M ultrafiltration apparatus using Ar or N_2 at 50 psi. In ultrafiltration determinations of micellar binding constants, it is desirable for the SDS and analyte concentrations to remain as constant as possible. In our experiments, through continuous stirring and replacement of the solution in the filtration chamber, the concentrations of SDS and retained species were not allowed to exceed 1.125 times their original concentrations. By monitoring the filtrate and retentate SDS concentrations, we confirmed previous reports[21,46] that SDS monomers can pass through a 1000 MWCO filter and that SDS aggregates are quantitatively retained. SDS concentrations were determined by extraction into chloroform with Azure A and measuring the absorbance of the chloroform layer at 636 nm.[47]

For phen, the micellar binding constant was determined by performing ultrafiltration on a series of solutions with a constant analyte concentration and an increasing SDS concentration. Filtrate phen concentrations were determined by spectrophotometric measurement at 264 nm ($\epsilon = 3.05 \times 10^4$ M^{-1} cm^{-1}).[48] For the cations $Tris^+$ and $Bis\text{-}Tris^+$, both analyte and SDS concentrations were held constant in a series of solutions with varying concentrations of added $NaNO_3$. Filtrate $Tris^+$ and $Bis\text{-}Tris^+$ concentrations were determined by titration with NaOH. The titration process was monitored potentiometrically, and the endpoints were determined using a Gran Plot analysis.[49] For all three analytes, control experiments were performed in the presence of 0.008 M SDS to verify that filtrate SDS concentrations did not interfere with the analysis.

The micellar binding constants K_X and K_{Na}^X are defined in the following equations, where X_f and X_f^+ are the unbound neutral and cationic species, respectively, and X_b and X_b^+ are the micelle-bound neutral and cationic species, respectively.

$$X_f + SDS_m \overset{K_X}{\rightleftharpoons} X_b \quad K_X = \frac{[X]_b}{[X]_f[SDS]_m} \tag{1}$$

$$X_f^+ + Na_b^+ \overset{K_{Na}^X}{\rightleftharpoons} X_b^+ + Na_f^+ \quad K_{Na}^X = \frac{[X^+]_b[Na^+]_f}{[X^+]_f[Na^+]_b} \tag{2}$$

Further explanation of these expressions is given in Supporting Information. The intrinsic retention of molecules in the absence of micelles in the ultrafiltration experiment requires the determination of the intrinsic retention ratio (I), which is also described in Supporting

(42) Charbit, G.; Dorion, F.; Gaboriaud, R. *J. Colloid Interface Sci.* **1985**, *106*, 265−268.
(43) Berthod, A.; Saliba, C. *Analusis* **1985**, *13*, 437−442.
(44) Wallace, R. M.; Katz, S. M. *J. Phys. Chem.* **1964**, *68*, 3890−3892.
(45) Varga, L. P.; Veatch, F. C. *Anal. Chem.* **1967**, *39*, 1101−1109.
(46) Hafiane, A.; Issid, I.; Lemordant, D. *J. Colloid Interface Sci.* **1991**, *142*, 167−178.
(47) Waters, J.; Taylor, C. G. The Colorimetric Estimation of Anionic Surfactants. In *Anionic Surfactants-Chemical Analysis*; Cross, J., Ed.; Marcel Dekker: New York, 1977.
(48) *Sadtler Standard Spectra, Ultraviolet Spectra*; Sadtler Research Laboratories: Philadelphia, 1975; Vol. 83, #22102.
(49) Rossotti, F. J. C.; Rossotti, H. *J. Chem. Educ.* **1965**, *42*, 375−378.

Information. The micellar binding constants and intrinsic retention ratios determined in this work are as follows: phen, $K_X = 140 \pm 10$, $I = 0.051$; $Tris^+$, $K_{Na}^X = 0.94 \pm 0.09$, $I = 0.043$; and Bis-$Tris^+$, $K_{Na}^X = 1.04 \pm 0.09$, $I = 0.074$. The micellar binding constant of $FeHDFB^+$, which was previously determined from ultrafiltration methods,[21] is $K_{Na}^X = 16$, and $I = 0.50$ if the original result is corrected for the extraneous retention of the Gouy−Chapman layer cations (see Supporting Information). The micellar binding constant of H^+ has been previously reported ($K_{Na}^X = 1$, $I = 0$).[21,46,50,51] As expected from its polyaromatic ring structure, phen has a very large K_X, indicating that it is strongly bound to micellar SDS. On the basis of this K_X value, phen is predicted to be ~75% bound to the micellar pseudophase when $[SDS]_m = 0.02$ M and ~95% bound when $[SDS]_m = 0.10$ M. For the $Tris^+$ and Bis-$Tris^+$ cations, $K_{Na}^X = 1$ within experimental error, indicating that there is no selectivity of the micellar surface for $Tris^+$ or Bis-$Tris^+$. This lack of selectivity simplifies calculations of micellar concentrations since $Tris^+$ or Bis-$Tris^+$ can simply be treated as additional Na^+ cations.

Calculations of Micellar Concentrations. Using the PPIE model and the measured values of K_X and K_{Na}^X reported above, we calculated the local concentrations of reactants in the micellar pseudophase. For additional background on the following equations and an outline of their derivation, refer to Supporting Information. For neutral molecules, the relationship between the micellar-bound and total concentrations of a species is

$$[X]_b = \frac{K_X[SDS]_m}{1 + K_X[SDS]_m}[X]_T = f_X[X]_T \quad (3)$$

As can be seen from eq 3, the fraction of X bound to the micellar phase (f_X) remains constant at a constant surfactant concentration. For cations under our experimental conditions, $[X^+]_b$ can be accurately approximated by

$$[X^+]_b = \frac{K_{Na}^X\beta[SDS]_m}{[M^+]_T + K_{Na}^X[X^+]_T + \beta[SDS]_m(K_{Na}^X - 1)}[X^+]_T = f_{X^+}[X^+]_T \quad (4)$$

where

$$[M^+]_T = [NaNO_3] + [SDS] + [Tris^+] + [Bis\text{-}Tris^+] \quad (5)$$

and β is a constant representing the fraction of micellar dodecyl sulfate headgroups with a bound cation. In our calculations, we used a value of $\beta = 0.8$. Note that for cations, f_X is a function of both the surfactant and inert counterion concentrations. For buffered cations, a slightly different expression is obtained:

$$[X^+]_b = \frac{K_{Na}^X\beta[SDS]_m}{[M^+]_T + K_{Na}^X[X^+]_f - \beta[SDS]_m}[X^+]_f = f_{X^+}[X^+]_f \quad (6)$$

Once the concentration of X bound to the micellar pseudophase has been calculated, $[X]_b$ is multiplied by a concentration factor to account for the smaller volume of the micellar pseudophase. Thus, the micellar concentration of X is given by

$$[X]_m = \frac{[X]_b}{[SDS]_m\bar{V}} \quad (7)$$

where $\bar{V}$ is the molar volume of the micellar pseudophase.[29] In our calculations, we used values of $\bar{V} = 0.25$ M^{-1} for phen and $\bar{V} = 0.15$ M^{-1} for all cationic species. For additional background on the values of β and $\bar{V}$ used in our calculations, refer to Supporting Information.

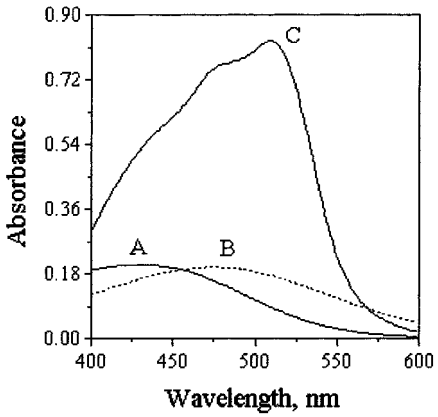

Figure 1. Absorption spectra of (A) $FeHDFB^+$ in aqueous solution, (B) the ternary complex intermediate product of reaction 9 in micellar SDS, and (C) the $Fe(phen)_3^{2+}$ product of reactions 8 and 10 in aqueous solution. Conditions: (A) $[Fe^{3+}]_{tot} = 7.4 \times 10^{-5}$ M, $[H_4DFB^+]_{tot} \cong 8.25 \times 10^{-5}$ M, 0.025 M $NaNO_3$, 0.0125 M Tris acetate buffer at pH 5.25; (B) same composition as A plus 2.3×10^{-4} M phen and 0.08 M SDS, 40 min after phen addition; (C) same composition as A plus 2.3×10^{-4} M phen and 3.75×10^{-2} M benzohydroxamic acid catalyst, 26 days after phen addition. All reactions were carried out at room temperature. Spectra were collected using a 1 cm path length cell.

Results

General Observations. Reaction of Ferrioxamine B and 1,10-Phenanthroline in Aqueous Solution. When ferrioxamine B ($FeHDFB^+$) and 1,10-phenanthroline (phen) are mixed in aqueous solution, an extremely slow, spontaneous conversion to $Fe(phen)_3^{2+}$ is observed:

$$Fe^{III}(HDFB)^+ + 3H^+ + 3phen + (Red) \rightarrow Fe^{II}(phen)_3^{2+} + H_4DFB^+ + (Ox) \quad (8)$$

Because of the large difference in the absorption spectra of $FeHDFB^+$ (Figure 1A) and $Fe(phen)_3^{2+}$ (Figure 1C), the reaction can be monitored spectrophotometrically. Although quantitative kinetic studies of reaction 8 were not performed, the progress of the reaction was periodically monitored for an extended period of time in order to verify the production of $Fe(phen)_3^{2+}$. Our qualitative observations indicate that the half-life of reaction 8 in aqueous solution ranges from ca. 3.5 days at pH 4.5 to ca. 6 days at pH 5.25. An interesting feature of reaction 8 is that the reduction of iron occurs in the absence of any additional iron(III)-reducing agent.

Preliminary investigations were conducted to determine other factors that might enhance the rate of reaction 8. Since the presence of bidentate chelators is known to catalyze ligand-exchange reactions of $FeHDFB^+$,[52,53] reaction 8 was carried out in the presence of acetohydroxamic acid (AHA) and benzohydroxamic acid (BHA). At pH 5.25, a 100-fold excess of either monohydroxamic acid ligand decreased the half-life of the reaction from 6 to 3.7 days. As in the aqueous $FeHDFB^+$−EDTA ligand-exchange reaction,[52] BHA was found to provide a slightly greater catalytic effect than AHA.

A greater rate acceleration effect can be achieved by introducing an effective reducing agent. Preliminary rate

(50) Bunton, C. A.; Ohmenzetter, K.; Sepulveda, L. *J. Phys. Chem.* **1977**, *81*, 2000−2004.
(51) Drummond, C. J.; Grieser, F. *J. Colloid Interface Sci.* **1989**, *127*, 281−291.
(52) Monzyk, B.; Crumbliss, A. L. *J. Inorg. Biochem.* **1983**, *19*, 19−39.
(53) Biruš, M.; Krznarić-Vohalski, G.; Kujundžic, N.; Nigovic, B.; Pribanić, M. *J. Inorg. Biochem.* **1998**, *70*, 253−263.

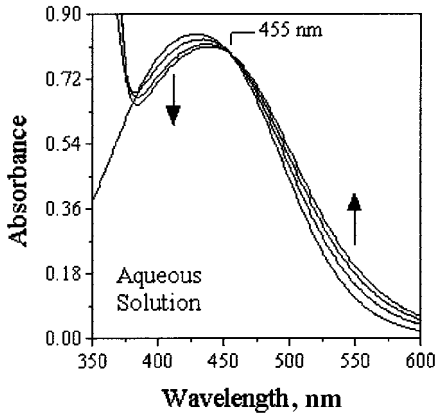

Figure 2. Equilibrium spectra in aqueous solution obtained for reaction 9 at various $[H^+]$ and a constant [phen]. A similar series of equilibrium spectra was obtained at a constant pH as the [phen] was varied. Arrows show the change in absorbance with increasing concentrations of phen (or H^+). The intense absorbances at <375 nm arise from $\pi-\pi^*$ transitions of the phen ligand. Conditions: $[Fe^{3+}]_{tot} = 3.05 \times 10^{-4}$ M, $[H_4DFB^+]_{tot} \cong 3.3 \times 10^{-4}$ M, $[phen]_{tot} = 0.0100$ M (except for the initial spectrum, where [phen] = 0), pH 5.42−4.38, 0.1 M $NaNO_3$, 0.05 M sodium acetate buffer, 25.0 ± 0.1 °C, 1 cm path length cell. Conditions for the phen titration (data not shown) are identical except that $[phen]_{tot} = 0-0.0100$ M and pH 4.54−4.76.

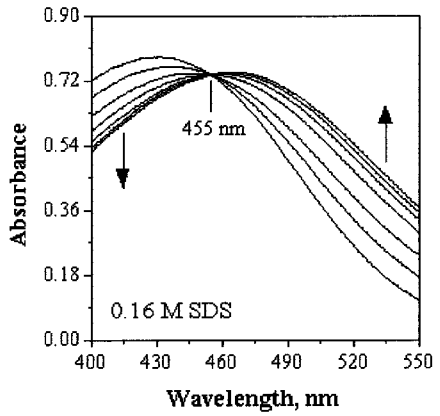

Figure 3. Equilibrium spectra obtained in 0.16 M SDS for the titration of reaction 9 with phen at a constant pH. A similar series of equilibrium spectra was obtained at a constant [phen] as the pH was varied. Arrows show the change in absorbance with increasing concentrations of phen (or H^+). Conditions: $[Fe^{3+}]_{tot} = 2.87 \times 10^{-4}$ M, $[H_4DFB^+]_{tot} \cong 3.3 \times 10^{-4}$ M, $[phen]_{tot} = 0-0.0125$ M, pH 6.30−6.36, 0.16 M SDS, 0.1 M $NaNO_3$, 0.05 M Bis-Tris buffer, 25.0 ± 0.1 °C, 1 cm path length cell. Conditions for the H^+ titration (data not shown) are identical except that $[phen]_{tot} = 0.0125$ M, pH 7.22−6.03, and 0.05 M Tris buffer was present.

measurements of reaction 8 were made in the presence of a mild reducing agent such as sodium ascorbate, hydroquinone, or hydroxylamine. Under our experimental conditions, none of these compounds are capable of reducing $FeHDFB^+$ in the absence of phenanthroline. However, when these reagents were added to reaction 8, they produced a significant rate acceleration. The magnitude of the rate acceleration varied with reducing agent in the order of ascorbate > hydroquinone > hydroxylamine. At pH 4.5, the presence of a 20-fold excess of ascorbate decreases the half-life of reaction 8 from ca. 3.5 days to 1 day.

At high concentrations of phen and lower-pH conditions, reaction 8 is observed to proceed in two distinct steps. A relatively rapid process approaches completion in <1 h, and the absorbance of the reaction mixture decreases slightly in the 375−450 nm range and increases slightly in the 460−600 nm region (see Figure 2). In a much slower subsequent stage, which occurs over a period of days, a large increase in absorbance occurs over the entire 400−600 nm range. The latter process eventually produces the characteristic $Fe(phen)_3^{2+}$ spectrum with a λ_{max} of 510 nm (Figure 1C). This biphasic kinetic behavior is consistent with a fast reaction (9) in which $FeHDFB^+$ and phen combine to form a ternary intermediate complex, followed by a slow reaction (10) in which the ternary intermediate reacts with additional phen to produce $Fe(phen)_3^{2+}$.

$$FeHDFB^+ + nH^+ + m\text{phen} \overset{K_1}{\rightleftharpoons} Fe(H_{1+n}DFB)(phen)_m^{1+n} \quad (9)$$

$$Fe(H_{1+n}DFB)(phen)_m^{1+n} + (3-n)H^+ + (3-m)\text{phen} \xrightarrow{+\text{reducing agent}} Fe(phen)_3^{2+} + H_4DFB^+ \quad (10)$$

Reaction of Ferrioxamine B and 1,10-Phenanthroline in Micellar SDS. When ferrioxamine B and phen are mixed in the presence of micellar SDS, a visible color change is observed within minutes. Depending on the pH and phen concentration, this reaction reaches completion within 5−40 min. As in aqueous solution, if the reaction mixture is allowed to stand, a much slower reaction occurs to produce $Fe(phen)_3^{2+}$. At pH 5.25, the slower reaction step (10) has a half-life of approximately 42 days. Qualitative observations indicate that the rate of reaction 10 is increased at lower pH values.

The absorbance changes observed for the first micellar reaction step are very similar to those observed in aqueous solution. The chief difference is that, in micellar solution, a greater amount of the intermediate product is formed so that a nearly complete conversion of $FeHDFB^+$ can be observed. Figure 1B shows the absorption spectrum of the micellar reaction mixture of 7.4×10^{-5} M $FeHDFB^+$ and 2.3×10^{-4} M phen at pH 5.25 after 40 min. As illustrated in Figure 1, the absorption spectrum of the ternary intermediate product (Figure 1B, $\lambda_{max} \approx 480$ nm) is considerably different from the absorption spectrum of the $FeHDFB^+$ reactant (Figure 1A, $\lambda_{max} = 428$ nm) or the $Fe(phen)_3^{2+}$ product (Figure 1C, $\lambda_{max} = 510$ nm).

Equilibrium Studies of Ternary Intermediate Formation. Because the half-lives of reactions 9 and 10 differ by several orders of magnitude, the equilibrium of the fast step (9) can be investigated independent of the slow step (10). Equilibrium studies were performed in both aqueous and 0.16 M SDS solutions. After the equilibration of reaction 9, absorption spectra were collected at different concentrations of H^+ and phen. When a series of these equilibrium spectra are overlaid, a number of similar features are evident (Figures 2 and 3). With each stepwise increase in [phen] or $[H^+]$, the spectra register a stepwise decrease in the $FeHDFB^+$ absorption band (430 nm) and a concomitant increase in the ternary intermediate absorption band (480 nm). In addition, each series of spectra in aqueous solution and micellar SDS possesses a clean isosbestic point at 455 nm. Two series of spectra, increasing $[H]^+$ at constant [phen] in aqueous solution and increasing [phen] at constant $[H]^+$ in 0.16 M SDS, are shown in Figures 2 and 3, respectively.

The presence of isosbestic points in these sets of spectra strongly suggests that only two light-absorbing species are present in the solution. This is supported by a rank analysis of the absorbance data, which found only two light-absorbing species in the 400−600 nm range. Thus, the equilibrium absorption spectra of the fast reaction (9) are consistent with a single process involving the direct conversion of reactants into a ternary intermediate product.

Kinetic Studies of Ternary Intermediate Formation in Micellar SDS. Kinetic measurements of the fast reaction (9) in micellar solution were performed under pseudo-first-order conditions of an excess of phen and a buffered pH. To verify a direct conversion of reactants to product in reaction 9, the rate of disappearance of $FeHDFB^+$ and the rate of formation of $Fe(H_{1+n}DFB)(phen)_m^{1+n}$ were monitored at 400 and 510 nm, respectively. The pseudo-first-order rate constants ($[FeHDFB^+] = 1.5 \times 10^{-4}$ M, [phen] = 5.0×10^{-3} M, [SDS] = 0.04 M, pH 4.75, $T = 25.0 \pm 0.1$ °C) were found to be identical to within one standard deviation: $(1.69 \pm 0.06) \times 10^{-2}$ s^{-1} at 400 nm and $(1.63 \pm 0.01) \times 10^{-2}$ s^{-1} at 510 nm. Extrapolation of stopped-flow spectrophotometric data obtained at 510 nm for the first 1 s to zero time yields an initial absorbance that is consistent with the average absorbance of the $FeHDFB^+$ and phen reactant solutions. Both the pseudo-first-order rate constants and the initial absorbance values are consistent with a direct conversion of $FeHDFB^+$ to $Fe(H_{1+n}DFB)(phen)_m^{1+n}$ in reaction 9.

Schwarzenbach Analysis of Ternary Intermediate Formation. The equilibrium constant for reaction 9 may be defined as shown in eq 11.

$$K_I = \frac{[Fe(H_{1+n}DFB)(phen)_m^{1+n}]}{[FeHDFB^+][H^+]^n[phen]^m} \qquad (11)$$

Since the preceding analyses indicate that only two light-absorbing species participate in reaction 9, the Schwarzenbach relationship[54−56] shown in eq 12 may be derived as

$$A_\infty = \frac{1}{K_I} \times \frac{A_i - A_\infty}{[H^+]^n[phen]^m} + A_f \qquad (12)$$

where A_i is the initial absorbance of $FeHDFB^+$, A_∞ is the equilibrium absorbance at each point in the titration, and A_f is the final absorbance when all $FeHDFB^+$ has been converted to $Fe(H_{1+n}DFB)(phen)_m^{1+n}$. From a series of plots of A_∞ vs $(A_i - A_\infty)/[H^+]^n[phen]^m$ (n = 0, 1, 2,..., and m = 0, 1, 2,...), it is possible to determine the stoichiometry and equilibrium constant for reaction 9. A fixed stoichiometry is demonstrated if a unique combination of n and m yields a linear plot of eq 12.

In both aqueous solution and micellar SDS, our experiments were designed to collect two series of equilibrium measurements: a series where [phen] was varied at a constant pH and a series where the pH was varied at a constant [phen]. When a Schwarzenbach analysis of the data obtained in the absence of SDS micelles was attempted, the variable pH and [phen] data did not fall on the same trendline for any values of n and m if the total concentration of phen was used in eq 12. However, if the concentration of *unprotonated* phen is used in the analysis, the data fall along the same trendlines. From this result, we conclude that protonated phen is unreactive toward $FeHDFB^+$. Under the higher-pH conditions of the micellar solutions, the amount of protonated phen is minimal and the total concentration of phen can be used in the generation of Schwarzenbach plots.

Panels A and B of Figure 4, respectively, show the aqueous solution and 0.16 M SDS A_∞ data at 525 nm obtained at variable [H^+] and [phen] plotted according to eq 12 when $n = m = 1$. For all other values of n and m, nonlinear plots were obtained. Two conclusions can be drawn from these results: (1) the same product is formed in both aqueous and micellar SDS solutions, and (2) one phen and one H^+ participate in reaction 9 to form the ternary intermediate product $Fe(H_2DFB)(phen)^{2+}$. The solid line in each figure represents a linear regression of the data from which a value of log $K_I = 6.96 \pm 0.07$ is obtained for aqueous solution and a value of log $K_I = 8.64 \pm 0.02$ is obtained for aqueous 0.16 M SDS.

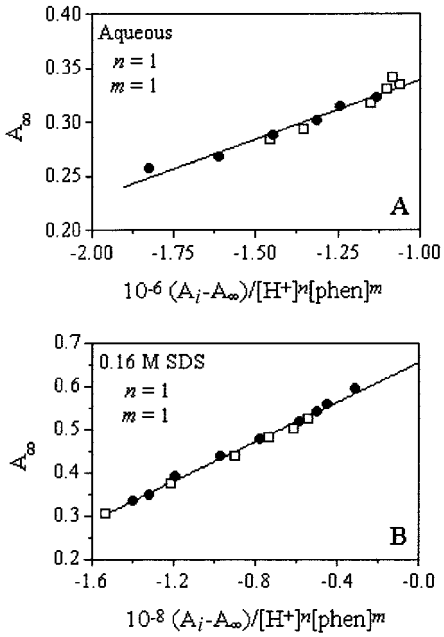

Figure 4. Schwarzenbach plots for reaction 9 in aqueous solution (A) and an aqueous 0.16 M SDS solution (B). Data collected at 525 nm for the titration with H^+ at a constant [phen] (●) and the titration with phen at a constant [H^+] (□). Solid lines represent a linear regression of the entire data sets from parts A and B. Absorbance data were recorded after equilibration of reaction 9 and plotted according to eq 12. In both A and B, linear plots were obtained only when $n = 1$ and $m = 1$, indicating that one H^+ and one phen participate in reaction 9 in the presence and absence of SDS micelles. For part A, only unprotonated phen was used to calculate the *x*-coordinates of data points (see text for a discussion). Regression parameters are as follows-(uncertainties represent 95% confidence limits). (A) Slope = $(1.09 \pm 0.17) \times 10^{-7}$, intercept = 0.449 ± 0.023, and $R^2 = 0.9534$. Log(1/slope) yields a log K_I(aq) value of 6.96 ± 0.07. Experimental conditions are given in Figure 2. (B) Slope = $(2.30 \pm 0.11) \times 10^{-9}$, intercept = 0.655 ± 0.010, and $R^2 = 0.9935$. Log(1/slope) yields a log K_I(mic) value of 8.64 ± 0.02. Experimental conditions are given in Figure 3.

Application of the Pseudophase Ion-Exchange (PPIE) Model. According to the PPIE model of micellar solutions, a micellar equilibrium constant for reaction 9 can be defined as

$$K_I^m = \frac{[Fe(H_2DFB)(phen)^{2+}]_m}{[FeHDFB^+]_m[H^+]_m[phen]_m} \qquad (13)$$

where the subscript m indicates the concentration in the micellar pseudophase. When micellar solutions influence reaction equilibria, the magnitude of the proximity effect is estimated by calculating the difference between K_I^m and K_I(mic), the value of K_I in micellar solution. Any difference between K_I^m and K_I(aq), the value of K_I in aqueous solution, is attributed to either a medium or compartmentalization effect.

Unfortunately, because of its instability, the micellar ion-exchange constant of $Fe(H_2DFB)(phen)^{2+}$ cannot be measured.

(54) Anderegg, G.; L'Eplattenier, F.; Schwarzenbach, G. *Helv. Chim. Acta* **1963**, *46*, 1409−1422.
(55) Raymond, K. N.; Müller, G.; Matzanke, B. F. *Top. Curr. Chem.* **1984**, *123*, 49−102.
(56) Caudle, M. T.; Cogswell, L. P., III; Crumbliss, A. L. *Inorg. Chem.* **1994**, *33*, 4759−4773.

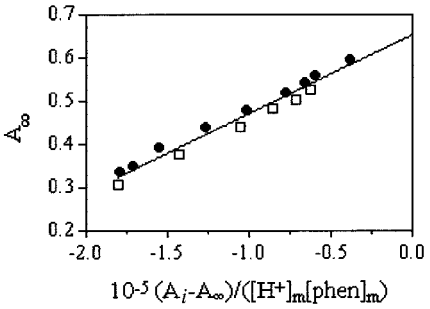

Figure 5. Schwarzenbach plot from Figure 4B using the micellar concentrations of H^+ and phen as calculated from eqs 3, 6, and 7. Symbols are defined in the Figure 4 caption. The solid line represents the linear regression of the entire data set. Regression parameters are as follows (uncertainties represent 95% confidence limits). Slope = $(1.83 \pm 0.21) \times 10^{-6}$, intercept = 0.654 ± 0.024, and $R^2 = 0.9654$. Log(1/slope) yields a log K_I^m value of 5.74 ± 0.05. Experimental conditions are given in Figure 3.

Nevertheless, a reasonable estimate of K_I^m can be obtained in the following fashion. If eq 13 is rearranged and eqs 4 and 7 are used to substitute for the micellar concentrations of Fe(H_2-DFB)(phen)$^{2+}$ and FeHDFB$^+$, the following expression may be obtained, where the subscript T denotes total concentration and *f* the fraction bound to the micellar pseudophase:

$$K_I^m[H^+]_m[phen]_m = \frac{f_{Fe(H_2DFB)(phen)^{2+}}[Fe(H_2DFB)(phen)^{2+}]_T}{f_{FeHDFB^+}[FeHDFB^+]_T} \quad (14)$$

Using eqs 3 and 4 and our experimental conditions, we calculated f_{phen} and f_{FeHDFB}, the fractions of phen and FeHDFB$^+$ bound to the micellar pseudophase, to be 0.96 and 0.92, respectively. Therefore, it is reasonable to assume that Fe(H_2-DFB)(phen)$^{2+}$ is almost entirely bound to the micellar phase, and to a first approximation, eq 15 holds

$$K_I^m[H^+]_m[phen]_m \cong \frac{[Fe(H_2DFB)(phen)^{2+}]_T}{[FeHDFB^+]_T} = \frac{A_i - A_\infty}{A_\infty - A_f} \quad (15)$$

Equation 15 can be rearranged to obtain a Schwarzenbach relationship similar to eq 12. Thus, a reasonable estimate of K_I^m may be obtained from a Schwarzenbach plot in which micellar concentrations of phen and H^+ are used. Figure 5 shows a Schwarzenbach plot for reaction 9 obtained with the micellar concentrations of phen and H^+ and with $n = m = 1$. The estimated value of log K_I^m, obtained from the slope of the regression line, is 5.74 ± 0.05. Although this is not an exact value, due to the uncertainty in the micellar binding of Fe(H_2-DFB)(phen)$^{2+}$, this estimate should be accurate within 10% of the true value.

Discussion

Overall Reaction. The reduction of FeHDFB$^+$ in the overall reaction (8) is quite remarkable considering the negative reduction potential of the FeHDFB$^+$ complex ($E_{1/2} = -0.483$ V vs NHE).[8] Our investigations with the mild reducing agents ascorbate, hydroquinone, and hydroxylamine demonstrate that, for these reducing agents, the presence of phen is necessary to achieve reduction. There are two probable means by which phen can facilitate the reduction process: (i) destabilizing the iron-(III) reactant through ternary complex formation with FeHDFB$^+$ prior to reduction or (ii) stabilization of the iron(II) product via complexation after reduction. In the first scenario, reduction is enabled through a positive shift in the reduction potential of the iron complex; in the second scenario, the complexation of iron(II) by phen provides the thermodynamic driving force necessary to facilitate the reduction of FeHDFB$^+$.

Since we have observed the Fe(H_2DFB)(phen)$^{2+}$ ternary complex intermediate in both aqueous and micellar SDS media, it is plausible to propose that phen facilitates FeHDFB$^+$ reduction through ternary complex formation. The enhanced rates of reaction 8 observed in the presence of monohydroxamate ligands and high H^+ concentrations are also consistent with this interpretation. However, beyond indicating that FeHDFB$^+$ dechelation precedes reduction, our results do not provide any additional insights into the nature of the reduction mechanism, which remains poorly understood.

In an independent study,[57] a crown ether was used to extract aqueous {FeHDFB$^+$, ClO_4^-} ion pairs into chloroform. For this two-phase system, reduction of FeHDFB$^+$ was observed only if phen was present during the extraction process. However, if FeHDFB$^+$ was extracted into chloroform and phen was added after the chloroform phase was separated from the aqueous layer, no reduction occurred. This intriguing result suggests that water facilitates the reduction process. The system may also be catalyzed by ambient fluorescent lighting.[57] Both of these results are consistent with the reported studies of the photoinduced and spontaneous reduction of Fe(phen)$_3^{3+}$ in aqueous solution.[58−64]

Effect of Micellar Aggregates. Our results clearly indicate that the micellar environment enhances formation of the ternary complex intermediate Fe(H_2DFB)(phen)$^{2+}$ (**II**). By comparing

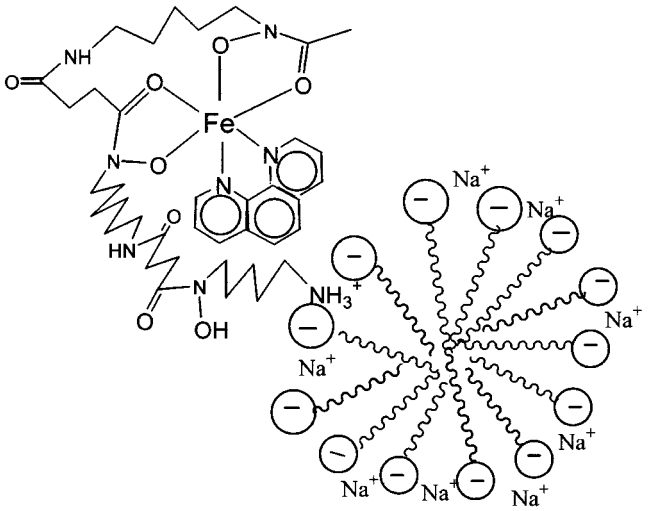

II - Fe(H_2DFB)(phen)$^{2+}$ on SDS micellar surface

the values of K_I (reaction 9; eq 11) determined in aqueous and micellar media, we found a micellar enhancement factor of $K_I(mic)/K_I(aq) = 10^{8.64}/10^{6.96} \cong 50$. Using the PPIE model, the magnitude of the proximity effect is calculated as $K_I(mic)/K_I^m = 10^{8.64}/10^{5.74} \cong 800$. Thus, while SDS micelles do stabilize the ternary intermediate (factor of 50), the stabilization is much less than would be predicted from the magnitude of the

(57) Caldwell, C. D. Ph.D. Dissertation, Duke University, Durham, NC, 1999.
(58) Wehry, E. L.; Ward, R. A. *Inorg. Chem.* **1971**, *10*, 2660−2664.
(59) David, P. G.; Wehry, E. L. *Mol. Photochem.* **1973**, *5*, 21−37.
(60) Nord, G.; Pedersen, B.; Bjergbakke, E. *J. Am. Chem. Soc.* **1983**, *105*, 1913−1919.
(61) Komadel, P.; Stucki, J. W. *Clays Clay Miner.* **1988**, *36*, 379.
(62) Monsted, O.; Nord, G. *Adv. Inorg. Chem.* **1991**, *37*, 381−397.
(63) Liu, R.-M.; Liu, D.-J.; Sun, A.-L. *Analyst* **1992**, *117*, 1767−1770.
(64) Pehkonen, S. *Analyst* **1995**, *120*, 2655−2663.

proximity effect (factor of 800). Clearly, either a strong medium or compartmentalization effect diminishes the stability of the ternary complex intermediate, $Fe(H_2DFB)(phen)^{2+}$, on the micelle surface by a factor of $K_I(aq)/K_I^m = 10^{6.96}/10^{5.74} \cong 16$.

Some insight into the nature of this medium or compartmentalization effect can be obtained by examining the interaction of $FeHDFB^+$ and phen with SDS individually. We have previously shown that the enhanced reactivity of $FeHDFB^+$ and H^+ in micellar SDS may be modeled by the proximity effect predicted from the PPIE model.[21] This suggests that the diminished stability of the ternary complex intermediate, $Fe(H_2DFB)(phen)^{2+}$, arises from a medium or compartmentalization effect involving the interaction of phen with SDS micelles. An examination of the H^+/phen interaction in the presence of SDS micelles supports this inference.

The fraction of phen bound to the micellar interface is calculated to be 0.95 under our conditions using eq 3. According to the PPIE model, the bound phen should experience the pH at the micellar interface. Using eqs 6 and 7, we found that an aqueous pH of 6.36 yields a micellar pH of 4.88. Using a pH of 4.88 and the aqueous pK_a of phen (4.93, 25 °C, $I = 0.1$ M),[22] we predicted phen to be ca. 50% protonated. However, the actual amount of protonated phen can be calculated from our experimental measurements of the change in bulk pH when phen is added to the SDS solution (Experimental Section: Equilibrium Measurements). When these pH measurements are used to calculate the amount of protonated Bis-Tris that is consumed by phen protonation, our measurements indicate that <10% of the phen is protonated at pH 6.36. This suggests that either the pK_a of phen on the micelle surface is shifted from 4.93 to 3.93 due to a medium effect[65,66] or ca. 80% of the phen is partitioned into the hydrophobic micellar interior where it is inaccessible to H^+. Either interpretation may be employed to explain the reduced reactivity of phen toward $FeHDFB^+$ in the presence of SDS micelles. Without a detailed knowledge of the exact microenvironment of phen in SDS micelles, it is difficult to predict which of these effects is the dominant influence on phen reactivity.

Implications for Microbial Model Systems. Our results reveal that iron can be removed from $FeHDFB^+$ in aqueous solution under mild pH conditions (pH 5.25) by a mild reducing agent (e.g., ascorbate) if a suitably strong iron(II) chelator is present. An analysis of this reaction suggests that iron release proceeds by ternary complex formation followed by reduction. The significance of these results is that they demonstrate that the reductive release of iron from $FeHDFB^+$ is feasible under relatively ordinary physiological conditions. Thus, this reaction system provides a possible model for siderophore iron release in vivo.

In addition, our results in micellar SDS illustrate how the cell membrane environment can enhance iron release from its siderophore complex. In our model system, the "binding" of $FeHDFB^+$, H^+, and phen to the micellar pseudophase acts as a crude mimic of a hypothetical molecular recognition site on the cell membrane surface. We have quantitatively demonstrated that this model produces a modest enhancement of ternary complex formation. If a more sophisticated form of molecular recognition were employed, one would expect the proximity effect to generate a greater enhancement of ternary complex formation.

According to the PPIE model, the proximity effect enhancement produced by our SDS micellar system was partially offset by an inhibitory medium or compartmentalization effect. Presumably, this design flaw could be corrected by choosing a different competing ligand that is localized in the same micellar microenvironment as $FeHDFB^+$ and H^+. Additional design improvements could produce favorable medium and compartmentalization effects. For example, if iron reduction could be localized in the micelle interior, the electron-transfer process could be enhanced by the reduced dielectric constant of this medium. Likewise, through the differential localization of the iron-free siderophore in the aqueous exterior and a hydrophobic iron complex in the membrane interior, a favorable compartmentalization effect could be realized. As these proposals suggest, our model system may provide guidance to the development of future siderophore iron release models.

Acknowledgment. Financial support from the National Science Foundation and the ACS Petroleum Research Fund is gratefully acknowledged.

Supporting Information Available: A background description of the ultrafiltration experiments and associated equations, calculations, and assumptions. This material is available free of charge via the Internet at http://pubs.acs.org.

IC0008621

(65) Underwood, A. L. *Anal. Chim. Acta* **1977**, *93*, 267−273.
(66) Fernández, M. S.; Fromherz, P. *J. Phys. Chem.* **1977**, *81*, 1755−1761.